Journal of Photochemistry and Photobiology A: Chemistry 223 (2011) 124–131

Contents lists available at SciVerse ScienceDirect

Journal of Photochemistry and Photobiology A: Chemistry

journal homepage: www.elsevier.com/locate/jphotochem

Conjugates of low-symmetry Ge, Sn and Ti carboxy phthalocyanines with glutathione caped gold nanoparticles: An investigation of photophysical behaviour

Nkosiphile Masilela, Tebello Nyokong*

Department of Chemistry, Rhodes University, Grahamstown 6140, South Africa

ARTICLE INFO

Article history:
Received 17 May 2011
Received in revised form 8 August 2011
Accepted 13 August 2011
Available online 22 August 2011

Keywords:
Monocarboxy phthalocyanine
Germanium
Titanium
Tin
Triplet quantum yields
Triplet lifetimes
Fluorescence quantum yields
Fluorescence lifetimes
Gold nanoparticle

ABSTRACT

This work reports on conjugation of low symmetry Ge (GeMCPc), Ti (TiMCPc) and Sn (SnMCPc) carboxy phthalocyanines with glutathione capped gold nanoparticles (GSH-AuNPs). The photophysical behaviour of the novel phthalocyanines–GSH-AuNPs conjugate was investigated and compared to the monocarboxy Pcs and to the mixture of Pc with GSH-AuNPs without a chemical bond. Blue shifting of Q band of the phthalocyanines was observed on linking to GSH-AuNPs. An improvement in triplet lifetimes was obtained for all the MPcs–GSH-AuNPs-linked conjugates compared to the MPcs alone. The highest triplet quantum yield of 0.75 and the longest triplet lifetime of 130 μs were obtained for the GeMCPc–GSH-AuNPs-linked conjugate. Fluorescence quantum yields and lifetimes were low for the conjugates due to quenching by the nanoparticles.

1. Introduction

Gold nanoparticles exhibit tunable optical properties, which depend on the size, shape and capping agent [1–4]. Phthalocyanines on the other hand are well known as photosensitizers for photodynamic therapy [5,6].

Conjugates of phthalocyanines and Au nanoparticles (AuNPs) have been reported for drug delivery applications [7–9]. Phthalocyanines conjugated to nanoparticles have demonstrated improved necrosis and/or apoptosis [8], hence our interest in this study. Gold nanoparticles are known to decrease the fluorescence lifetime of the Pc molecule, due to energy transfer from the Pc molecule to the attached AuNP, though the phase transfer agent (tetraoctylammonium bromide, TOABr), is also known to decrease the fluorescence lifetimes of free Pcs [9]. Energy transfer from the photoexcited phthalocyanines to the gold nanoparticles occurs in the picosecond time scale ~3 ps [10]. In another study [11], gold nanoparticles were found not to quench the fluorescence of cobalt tetramino phthalocyanine, whereas silver nanoparticles did. Thus it is clear from the literature that the fluorescence behaviour of phthalocyanines alone or in the presence of AuNPs depends on the nature of the macrocycle.

Cook and coworkers reported on a direct linkage of zinc phthalocyanines on gold nanoparticles via a peripheral thiol [7,8]. Recently a report by Kotiaho et al. presented the interaction of unmetallated phthalocyanines substituted with thioacetate groups to gold nanoparticles (AuNPs) [10]. However peripherally thiol-substituted Pcs are difficult to synthesize due to possible formation of disulfide bonds. In this work we report on a new approach of forming conjugates between AuNPs and phthalocyanines which do not contain thiol groups. This is achieved by using glutathione as a peptide intermediate for coupling, since it has a thiol to couple to the AuNPs and a free amino group to bind to low symmetry phthalocyanine complexes containing one reactive carboxylic acid group. Unmetallated phthalocyanines or those containing zinc in the central cavity have been well researched. Hence in this work, we use the less common Ti, Ge and Sn as central metals for the monocarboxy phthalocyanines. The effects of the central metal on the photophysical behaviour (triplet state quantum yields and lifetimes as well as fluorescence quantum yields and lifetimes) of the Pcs alone, and when in a mixture with AuNPs (represented as MPc–GSH-AuNPs-mixed) or linked to AuNPs (represented as

* Corresponding author. Tel.: +27 46 6038260; fax: +27 46 6225109.
E-mail address: t.nyokong@ru.ac.za (T. Nyokong).

1010-6030/$ – see front matter © 2011 Elsevier B.V. All rights reserved.
doi:10.1016/j.jphotochem.2011.08.009

MPc–GSH-AuNPs-linked) will be studied. This is the first study of triplet state quantum yields and lifetimes of MPc–AuNPs conjugates.

2. Experimental and methods

2.1. Materials

Sodium borohydride, *N*,*N*-dimethylformamide (DMF), methanol (MeOH), tetrahydrofuran (THF), and toluene were purchased from Saarchem. Glutathione (98%), tetraoctylammonium bromide (TOABr) (98%), dicyclohexylcarbodiimide (DCC), NaOH, potassium bromide, aluminium oxide (WN-3:neutral) and gold (III) chloride trihydrate (99.9%) were purchased from Sigma–Aldrich.

2.2. Synthesis of nanoparticles

2.2.1. Synthesis of TOABr stabilized AuNPs

Gold nanoparticles were synthesized according to the reported procedure [12] using TOBr as a stabilizing agent. Briefly, gold (III) chloride trihydrate in aqueous solution (25 mM, 10 mL) was stirred for 5 min in the presence of a toluene solution of TOABr (85 mM, 15 mL) until all of the gold chloride was transferred to the organic phase. The reducing agent, $NaBH_4$, in an aqueous solution (36 mM, 10 mL) was added drop-wise to the solution for 10 min. After the addition of $NaBH_4$, the mixture was stirred vigorously for 25 min until a deep purple colour was observed. The purple organic phase which contains the nanoparticles was separated and washed with water.

2.2.2. Synthesis of GSH capped AuNPs

GSH stabilized AuNPs were synthesized according to the previously reported procedure [1] with modification. Briefly GSH was dissolved in ethanol:water (1:1) to make a 50 mM solution, which was flushed with argon for 45 min before use. The GSH solution was then added to an equal volume ratio of TOABr stabilized AuNPs in toluene and mixed. The mixture was stirred under argon for 12 h for the ligand exchange to take place. After the reaction was complete, the water soluble GSH capped nanoparticles were separated by centrifugation. A 90% product yield was achieved.

2.2.3. Conjugation of GSH capped AuNPs to low symmetry carboxy Ge (2), Ti (3) and Sn (4) phthalocyanines

The syntheses of low symmetry monocarboxy phthalocyanines of germanium (GeMCPc, 2), titanium (TiMCPc, 3) and tin (SnMCPc, 4) were recently reported [13]. The monocarboxy Pc (10 mg) was firstly dissolved in DMF (10 mL), then 30 mg DCC was added to convert the carboxylic group (–COOH) of the Pc into an active carbodiimide ester group. The mixture was left to stir at room temperature under a nitrogen atmosphere for 48 h. After this time, 20 mL GSH-AuNPs in water:DMF (1:1) solvent mixture was added to the activated Pc and the mixture was stirred for 48 h to allow for conjugation of the Pc to the GSH-AuNP to take place. The conjugate was separated from un-conjugated nanoparticles using alumina chromatographic column, using 0.1 M NaOH:methanol (1:1) to elute the nanoparticles followed by DMF:methanol (5:1) to elute the conjugate. In order to ensure that the conjugate was free of unreacted Pcs and AuNPs, the solution of the conjugates was run through a size-exclusion column (Bio-Beads S-X1 from Bio-Rad) using THF:methanol (2:1) as an eluent. And 70% of the product yield was obtained.

2.3. Equipment

UV–visible spectra were recorded on a Shimadzu 2550 UV-Vis spectrophotometer. Fluorescence excitation and emission spectra were recorded on a Varian Eclipse spectrofluoremeter. IR spectra (KBr pellets) were recorded on a Perkin-Elmer spectrum 2000 FTIR spectrometer. Transmission electron microscope (TEM) images were obtained using a JEOL JEM 1210 transmission electron microscope at 100 kV accelerating voltage. TEM samples were prepared by placing a drop of conjugates or nanoparticles solution on the sample grid and allowing it to dry before measurements.

Fluorescence lifetimes were measured using a time correlated single photon counting setup (TCSPC) (FluoTime 200, Picoquant GmbH) with a diode laser (LDH-P-670 with PDL 800-B, Picoquant GmbH, 670 nm, 20 MHz repetition rate, 44 ps pulse width). Fluorescence was detected under the magic angle with a peltier cooled photomultiplier tube (PMT) (PMA-C 192-N-M, Picoquant) and integrated electronics (PicoHarp 300E, Picoquant GmbH). A monochromator with a spectral width of about 8 nm was used to select the required emission wavelength band. The response function of the system, which was measured with a scattering Ludox solution (DuPont), had a full width at half-maximum (FWHM) of 300 ps. All luminescence decay curves were measured at the maximum of the emission peak and lifetimes were obtained by deconvolution of the decay curves using the FluorFit software program (PicoQuant GmbH, Germany). The support plane approach [14] was used to estimate the errors of the decay times.

Laser flash photolysis experiments were performed with light pulses produced by a Quanta-Ray Nd: YAG laser providing 400 mJ, 9 ns pulses of laser light at 10 Hz, pumping a Lambda-Physik FL3002 dye (Pyridin 1 dye in methanol). Single pulse energy ranged from 2 to 7 mJ. The analyzing beam source was from a Thermo Oriel xenon arc lamp, and a photomultiplier tube was used as a detector. Signals were recorded with a digital real-time oscilloscope (Tektronix TDS 360). The solutions (absorbance ~1.5 at the Q band) for triplet quantum yields and lifetimes were introduced into a 1 cm path length UV/visible spectrophotometric cell, de-aerated using argon (bubbled for 30 min) and irradiated at the Q band maxima with laser flash photolysis equipment described above. The triplet lifetimes were then determined by exponential fitting of the kinetic curves using the program OriginPro 8.0.

X-ray powder diffraction (XRD) patterns were recorded on a Bruker D8, Discover equipped with a proportional counter, using Cu-K radiation (=1.5405 Å, nickel filter). Data were collected in the range from $2\theta = 5^\circ$ to 100°, scanning at $1^\circ\,min^{-1}$ with a filter time-constant of 2.5 s per step and a slit width of 6.0 mm. Samples were placed on a silicon wafer slide. The X-ray diffraction data were treated using the freely available Eva (evaluation curve fitting) software. Baseline correction was performed on each diffraction pattern by subtracting a spline fitted to the curved background.

2.4. Photophysical parameters (fluorescence and triplet quantum yield determination)

Fluorescence quantum yields (Φ_F) were determined by comparative method [15] (Eq. (1))

$$\Phi_F = \Phi_{F(Std)} \cdot \frac{F.A_{Std}.n^2}{F_{Std}.A.n^2_{Std}} \quad (1)$$

where F and F_{Std} are the areas under the fluorescence curves of the MPc derivatives and the reference, respectively. A and A_{Std} are the absorbances of the sample and reference at the excitation wavelength, and n and n_{Std} are the refractive indices of solvents used for the sample and standard, respectively. ZnPc in DMSO was used as a standard, $\Phi_F = 0.2$ [16]. At least three independent experiments were performed for the quantum yield determinations. Both the sample and the standard were excited at the same relevant wavelength.

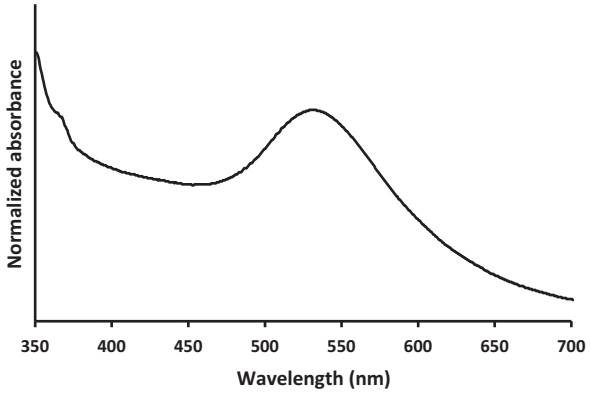

Fig. 1. Ground state electronic absorption spectra of GSH-AuNP in water.

Triplet quantum yields were determined using a comparative method based on triplet decay, using Eq. (2):

$$\Phi_T^{Sample} = \Phi_T^{Std} \frac{\Delta A_T{}^{Sample} \varepsilon_T{}^{Std}}{\Delta A_T{}^{Std} \varepsilon_T{}^{Sample}} \quad (2)$$

where A_T^{Sample} and A_T^{Std} are the changes in the triplet state absorbance of the sample and the standard, respectively. ε_T^{Sample} and ε_T^{Std} are the triplet state extinction coefficients for the sample and standard, respectively. Φ_T^{Std} is the triplet state quantum yield for the standard. Unsubstituted ZnPc was used as a standard, Φ_T^{Std} = 0.58 for ZnPc in DMF [17].

ε_T^{sample} and ε_T^{Std} were determined from the molar extinction coefficients of their respective ground singlet state (ε^{Sample} and ε_S^{Std}), the changes in absorbances of the ground singlet states (ΔA^{Sample} and ΔA_S^{Std}) and changes in the triplet state absorptions, (ΔA_T^{Sample} and ΔA_T^{Std}) according to Eqs. (3a) and (3b):

$$\varepsilon_T^{sample} = \varepsilon^{Sample} \frac{\Delta A^{Sample}}{\Delta A^{Sample}} \quad (3a)$$

$$\varepsilon_T^{Std} = \varepsilon_S^{Std} \frac{\Delta A_T^{Std}}{\Delta A_S^{Std}} \quad (3b)$$

3. Results and discussion

3.1. Synthesis and spectral characterisation

3.1.1. GSH-AuNPs

Glutathione capped AuNPs, Scheme 1 (1), were prepared from the TOABr stabilized nanoparticles. Glutathione was selected as a tri-peptide of interest in this work because of its free cystenyl thiol that has a high binding affinity to gold [18]. However oxidation is a major problem with solutions of GSH because of the free cysteinyl thiol present in the peptide sequence. GSH was kept in its reduced state during ligand exchange reactions by carefully evacuating the solution containing GSH to get rid of excess oxygen, and saturating with argon gas, followed by sealing in an inert environment. This prevents oxidation of GSH to oxidized glutathione (GSSG). After TOABr ligand exchange with glutathione, the nanoparticles were highly soluble in aqueous solution suggesting that a strong interaction with GSH has occurred. Fig. 1 shows UV–vis spectra of AuNPs after ligand exchange with GSH. The surface plasmon resonance (SPR) band for AuNP absorption was observed at 522 nm for the GSH-AuNPs in water (Fig. 1).

The nanoparticles were characterised by TEM (Fig. 2(a)). The shape of the AuNPs was found to be spherical from TEM images. The size of the AuNPs was determined using X-ray powder diffraction (XRD) [19], Fig. 1 (Supplementary data, Fig. 1), and the Debye–Scherrer Eq. (4):

$$d(\overset{0}{A}) = \frac{k\lambda}{\beta Cos\theta} \quad (4)$$

where k is an empirical constant equal to 0.9, λ is the wavelength of the X-ray source (1.5405 Å), β is the full width at half maximum of the diffraction peak, and θ is the angular position of the peak. The size of the GSH-AUNPs was determined to be 5.2 nm using Eq. (4).

3.1.2. MPc–GSH-AuNPs conjugates

The nanoparticles were coupled to low symmetry metallophthalocyanine of GeMCPc (2), TiMCPc (3) and SnMCPc (4) resulting in MPc–GSH-AuNPs conjugates (5). The Pcs are conjugated via the amine group of GSH and the free carboxylic acid of the Pc using DCC as a coupling agent. The conjugates are represented as GeMCPc–GSH-AuNPs-linked, TiMCPc–GSH-AuNPs-linked and SnMCPc–GSH-AuNPs-linked.

The TEM image of GSH-AuNPs in Fig. 2(a) shows dispersed nanospherically shaped particles. A clear indication of agglomeration was observed from the TEM images of the GeMCPc–GSH-AuNPs-linked (Fig. 2b), TiMCPc–GSH-AuNPs-linked (Fig. 2c) and SnMCPc–GSH-AuNPs-linked (Fig. 2d). The aggregation could be a result of the method used in preparing samples for TEM since phthalocyanines readily form aggregates. The GeMCPc–GSH-AuNPs-linked (Fig. 2b) displayed a different form of agglomerates as compared to the TiPc and SnPc conjugates. For GeMCPc–GSH-AuNPs-linked (Fig. 2b) isolated circular islands of agglomerates were observed.

The XRD spectra of the conjugates (GeMCPc–GSH-AuNPs-linked, TiMCPc–GSH-AuNPs-linked and SnMCPc–GSH-AuNPs-linked), the unconjugated MPc complexes and the GSH-AuNPs alone are shown in Fig. 1 (Supplementary data, Fig. 1). The XRD parameters are listed in Table 1. The gold nanoparticles show typical XRD spectra [20]. Broadening of the XRD peaks was observed for all the monocarboxy Pc complexes suggesting that the complexes are present in a amorphous form as shown in Fig. 1A (spectra (a), Supplementary data, Fig. 1). For TiMCPc and SnMCPc, the peak near $2\theta = 25^\circ$ is typical of amorphous phase in phthalocyanines [21]. The XRD spectrum of the MPcs–GSH-AuNPs-linked shows a number of additional peaks corresponding to the GSH-AuNPs when compared to the MPcs alone. The XRD spectra of these conjugates show the presence of both the MPc and GSH-AuNPs peaks, but not necessarily conjugation. It has been reported that both the degree of crystallization and the interplanar space changes, imply a new crystal form or a new compound in phthalocyanines [22]. Thus the change in 2θ angles and d-spacings including the appearance of new XRD peaks confirms a new crystal formation of the phthalocyanine or a new compound, hence confirms conjugation. For the GeMCPc–GSH-AuNPs-linked conjugate, Fig. 1A (spectrum (b), Supplementary data, Fig. 1), two peaks appeared corresponding to the GSH-AuNPs at 38.2° and 44.4° (Table 1). The peaks are typical of GSH-AuNPs and the peaks near 65° are due to both the GSH-AuNPs and Pcs. Sharp peaks were observed for the TiMCPc–GSH-AuNP-linked conjugate, Fig. 1B (spectrum (b), Supplementary data, Fig. 1), in addition to GSH-AuNPs peaks suggesting that a crystalline bulky structure may have formed. The nanoparticle peaks appear with lower intensity at 38.2° and 44.7°. Broadening was observed for the peaks at 64.6° and 77.8° suggesting coupling of the TiMCPc and the nanoparticles. Less peak broadening was observed for the SnMCPc–GSH-AuNPs-linked conjugate, Fig. 1C (spectrum (b), Supplementary data, Fig. 1), compared to GeMPc–GSH-AuNPs-linked conjugates. A new broad peak was observed at an angle 17.7° which might be the shifted SnMCPc peak. The other six peaks observed at 38.1°, 44.4°, 64.5°, 77.6°, 81.8° and 98.4° (Table 1) correspond to the GSH-AuNPs peaks.

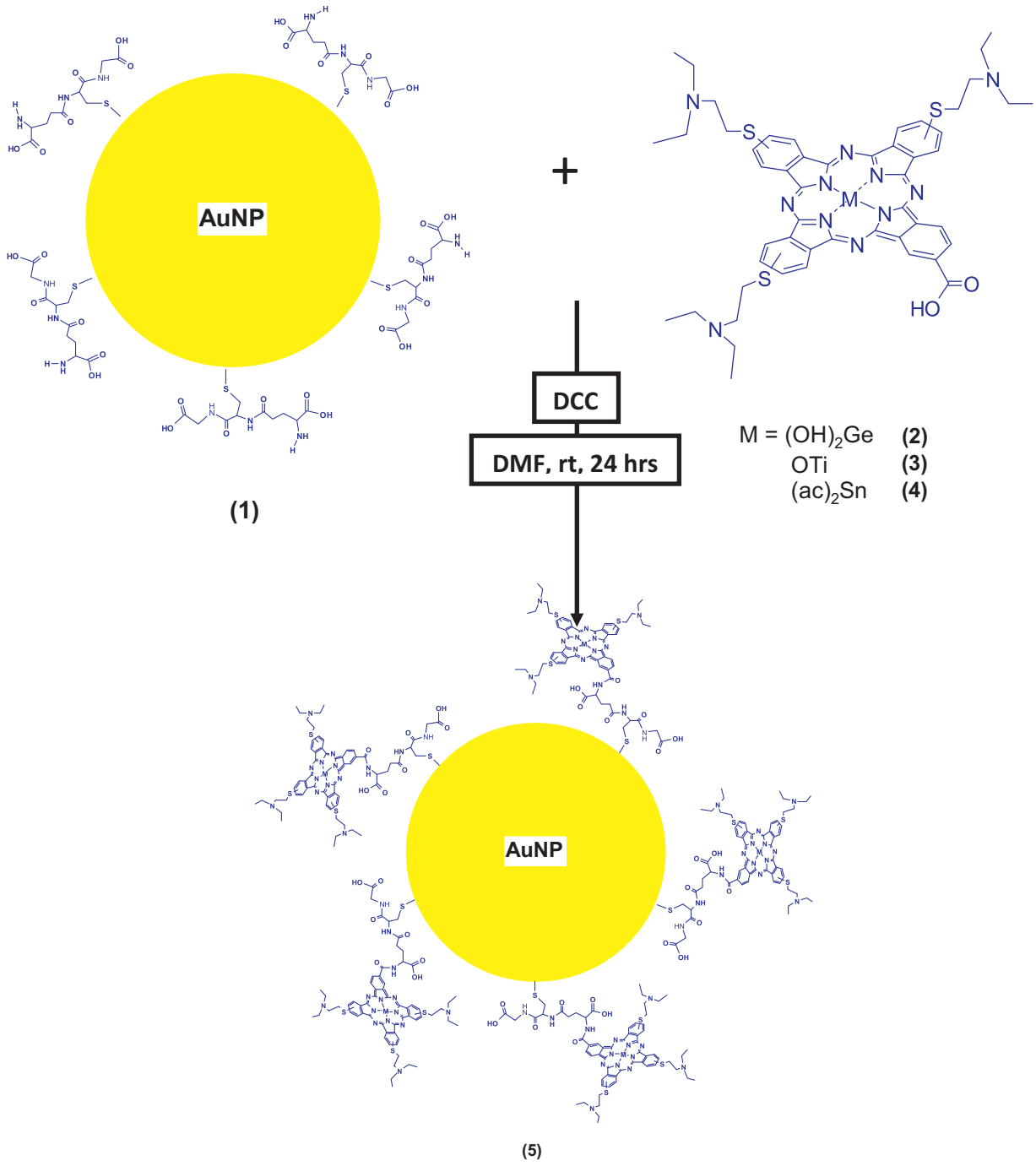

Scheme 1. Schematic representation of the coupling glutathione caped gold nanoparticles (**1**) to low symmetry monocarboxy metallophthalocyanines (**2–4**).

No drastic UV–visible spectral changes (Fig. 3) of the Q-band maxima for all the MPc complexes were observed before and after the low symmetry phthalocyanine complexes were mixed with the GSH-AuNPs, indicating no interaction. A 1–3 nm shift was observed as a result of change in the environment after mixing MPcs with GSH-AuNPs. A broad absorption band was observed at the region between 450 and 550 nm where the SPR band of AuNPs occurs. Significant blue shifting in spectra was observed for all the complexes after they were chemically coupled to the GSH-AuNPs. All MPc–GSH-AuNPs-linked conjugates showed large shift in the Q band compared to MPc alone or mixed with GSH-AuNPs without a chemical bond (Fig. 3) confirming successful coupling to the nanoparticles. In phthalocyanine chemistry, blue shifting and broadening of the Q band in most cases is explained as a result of coplanar association of phthalocyanine rings progressing from monomers leading to aggregates. The most likely aggregates in phthalocyanines are the so called H aggregated (face to face) which result in blue shifting or broadening of the spectra. However in the case of these MPc–GSH-AuNPs-linked conjugates, there is blue shifting but the shape of the Q band is not typical of aggregation. The blue shifting in phthalocyanines is usually attributed to the presence of electron withdrawing ligands [23] due to an increase in the highest occupied molecular orbital (HOMO) – lowest unoccupied molecular orbital (LUMO) gap of the MPcs. The blue shift observed in Fig. 3 has been reported before when phthalocyanines are linked to AuNPs [7], and suggests π electron deficiency of the Pcs

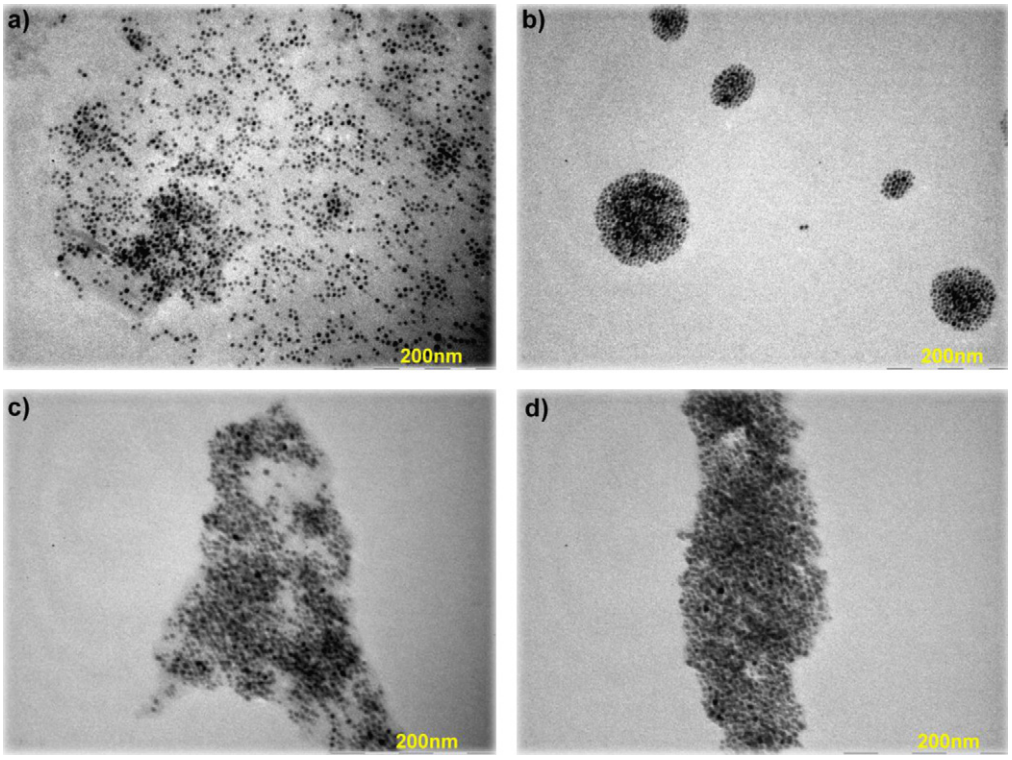

Fig. 2. Transmission electron microscope (TEM) images of GSH capped AuNPs alone (a), or linked to GeMCPc (b), TiMCPc (c) and SnMCPc (d).

following coordination of GSH-AuNPs. There is narrowing of the Q band following coordination of Pcs to AuNPs, suggesting reduction in aggregation in solution. The attachment of bulky GSH-AuNPs to the phthalocyanine is expected to reduce face to face aggregation.

The FTIR spectra (Fig. 4) also served as a qualitative tool to confirm conjugation of the MPcs to the GSH-AuNPs. The sharp bands observed in all the top (a) IR spectra at 3342 cm^{-1} in Fig. 4A, 3332 cm^{-1} in Fig. 4B and 3420 cm^{-1} in Fig. 4C are an indication of the presence of an amide linkage resulting from the –NH stretching respectively, hence confirms the formation of conjugate. The GSH-AuNPs on their own have amide bonds hence are expected to show C=O vibrations. However the IR spectra of GSH-AuNPs showed very broad peaks in the 3300–3500 cm^{-1} region (Fig. 2 Supplementary data), which are quite different from the resolved bands observed following coordination. Thus the IR by itself may not unequivocally prove the amide bond between GSH and MPC complexes, but the refinement in the –NH vibrations shows that a change has occurred. For the GeMCPc–GSH-AuNPs-linked conjugate (Fig. 4A) the C=O stretching was observed at 1593 and 1538 cm^{-1}, for the TiMCPc–GSH-AuNPs-linked (Fig. 4B) conjugate at 1600 and 1545 cm^{-1} and for the SnMCPc–GSH-AuNPs-linked (Fig. 4C) conjugate at 1634 and 1519 cm^{-1}. These bands are also present in GSH-AuNPs at 1593 and 1538 cm^{-1}, (Fig. 2 Supplementary data). The IR spectra of Pcs alone all show sharp doublet C–H stretching at 2964 cm^{-1}, Fig. 4A (b), 2963 cm^{-1}, Fig. 4B (b), and 2970 cm^{-1}, Fig. 4C (b), these are due to the aliphatic C–H of the methyl and methylene groups of the peripheral ligands. All other peaks below the region of 1500 cm^{-1} were observed in the conjugate and are in the phthalocyanine figure print region.

3.2. Photophysical properties

3.2.1. Fluorescence behaviour

Fig. 5 shows the absorption, fluorescence excitation and emission spectra of the MPcs–GSH-AuNPs-linked conjugates. The GeMCPc–GSH-AuNPs-linked (Fig. 5A) absorption spectrum is broader than the excitation spectrum, most likely due to aggregation since aggregates do not fluoresce. The fluorescence emission

Table 1
XRD parameters for the GSH-AuNPs, monocarboxy phthalocyanines (GeMCPc (2), TiMCPc (3) and SnMCPc (4)) and their conjugate with GSH-AuNPs.

Compound	D-spacing of peaks and $2\theta^{\circ}$ values								
GeMCPc	d-spacing	1.49	1.19						
	$2\theta^{\circ}$	62.3	80.8						
GeMCPc–GSH-AuNPs-linked	d-spacing	2.36	2.04	1.45	1.23	1.17			
	$2\theta^{\circ}$	38.2	44.4	64.3	77.7	82.1			
TiMCPc	d-spacing	3.71	1.48	1.19					
	$2\theta^{\circ}$	23.9	62.9	80.2					
TiMCPc–GSH-AuNPs-linked	d-spacing	5.78	5.13	3.82	3.10	2.36	2.03	1.44	1.23
	$2\theta^{\circ}$	15.3	17.3	23.3	28.8	38.2	44.7	64.6	77.8
SnMCPc	d-spacing	3.48	1.48	1.20					
	$2\theta^{\circ}$	25.6	62.9	79.8					
SnMCPc–GSH-AuNPs-linked	d-spacing	5.00	2.36	2.04	1.44	1.23	1.18	1.02	
	$2\theta^{\circ}$	17.7	38.1	44.4	64.5	77.6	81.8	98.4	
GSH-AuNPs	d-spacing	2.35	2.04	1.44	1.23	1.18	1.02		
	$2\theta^{\circ}$	38.2	44.3	64.7	77.7	81.8	98.2		

Table 2
Fluorescence and photophysical parameters of GeMCPc (2), TiMCPc (3) and SnMCPc (4) mixed and linked to GSH capped AuNPs in DMF.

Complex	Q-band λ_{Abs} (nm)	Φ_T	Φ_F	τ_T (μs)	Fluorescence lifetimes τ_F (ns)			
					τ_{F1}	Amplitude	τ_{F2}	Amplitude
GeMCPc	695	0.70	0.09	70	1.61	1		
GeMCPc–GSH-AuNPs-mixed	693	0.72	<0.01	110	1.10	0.85	0.64	0.15
GeMCPc–GSH-AuNPs-linked	680	0.75	<0.01	130	1.0	0.90	0.53	0.10
TiMCPc	734	0.63	0.11	57	1.84	1		
TiMCPc–GSH-AuNPs-mixed	733	0.64	0.03	62	1.20	0.80	0.93	0.20
TiMCPc–GSH-AuNPs-linked	711	0.65	<0.01	95	1.40	0.95	0.80	0.05
SnMCPc	720	0.65	0.14	64	2.35	1		
SnMCPc–GSH-AuNPs-mixed	720	0.66	0.02	61	1.50	0.79	0.84	0.31
SnMCPc–GSH-AuNPs-linked	702	0.67	<0.01	80	1.70	0.96	0.74	0.04

spectra are mirror images of the excitation spectra for all conjugates. Table 2 compares the fluorescence quantum yields (Φ_F) of the conjugates (MPcs–GSH-AuNPs-linked) to the low symmetry MPcs alone, and to MPc mixed with GSH-AuNPs with no linking agent. Lower fluorescence quantum yields of <0.01 were observed for all the linked complexes. For mixed complexes (MPc–GSH-AuNPs-mixed), the values were marginally better than for the linked (MPc–GSH-AuNPs-linked) conjugates with the exception of GeMCPc–GSH-AuNPs-linked, where the values were the same. The drastic decrease of the fluorescence quantum yields after conjugation is most likely due to phthalocyanine fluorescence quenching by gold nanoparticles. It has been documented that gold nanoparticle quench phthalocyanine fluorescence [9,10]. However, it is also possible that in addition, the heavy atom effect of the GSH-AuNPs results in enhanced intersystem crossing to the triplet state. Thus the two processes may be contributing to the low Φ_F values. The latter factor would result in increased triplet yield quantum yields which will be discussed below.

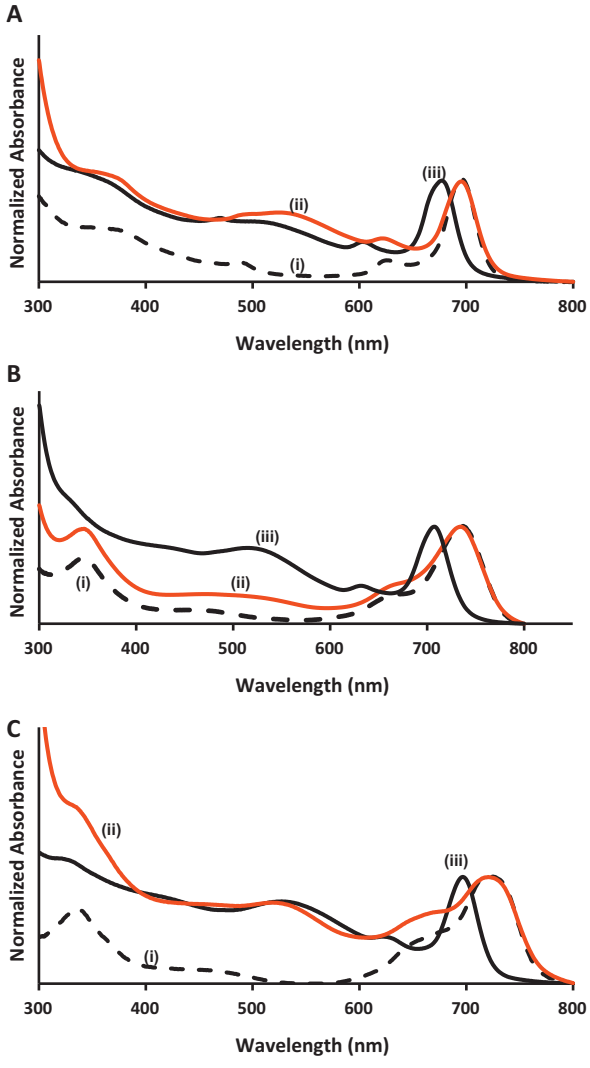

Fig. 3. Ground state absorption spectra of GeMCPc (A), TiMCPc (B) and SnMCPc (C); Pc alone (i), mixed with nanoparticles (ii) and linked (iii) in DMF.

Fig. 6 shows time-resolved fluorescence decay curve of TiMCPc–GSH-AuNPs-linked in DMF, indicating a bi-exponential decay. Free Pcs showed only one lifetime in Table 2. The existence of two components in the fluorescence decay of the Pcs in the absence of GSH-AuNPs has been reported and was attributed to the nature of substituents [7] or to the formation of ground-state dimers which can quench the monomer fluorescence, leading to a quenched and unquenched lifetime [24]. The longer (unquenched) lifetime is attributed to the monomer and the shorter lifetime is attributed to quenched lifetime of the dimer [25]. In this work one lifetime was observed for Pc alone, but two lifetimes appear for the conjugates, Table 2. The fluorescence lifetimes of the free Pc is decreased for both the conjugates (MPc–GSH-AuNPs-linked) and the mixed (MPc–GSH-AuNPs-mixed, without a chemical bond), due to the quenching of fluorescence discussed above and reported before [25].

3.2.2. Triplet state parameters

The triplet decay curve for SnMCPc–GSH-AuNPs-linked conjugate shown in Fig. 7 obeyed second order kinetics. This is typical of MPc complexes at high concentrations (>1×10^{-5} M) [24] due to the triplet–triplet recombination. The highest triplet quantum yield (Φ_T) of 0.70 obtained for the GeMCPc, followed by the SnMCPc with Φ_T = 0.65 and TiMCPc with Φ_T = 0.63 in DMF. It is important to note that the triplet states of MPc complexes are quenched by oxygen [26], hence de-oxygenation is important for the accurate determination of triplet quantum yields and lifetimes. De-oxygenation was done in this work using argon as stated in Section 2. There was an insignificant increase in triplet quantum yields for all the mixed (MPc–GSH-AuNPc-mixed complexes, without a chemical bond). A slight improvement in triplet yields was observed for MPc–GSH-AuNPs-linked compared to the MPc alone, suggesting that the GSH-AuNPs encourages intersystem crossing to the triplet state. However, the increase is very small, confirming that the low Φ_F values discussed above are influenced more by quenching by AuNPs than by intersystem crossing (ISC). ISC would result in a larger increase in Φ_T values than observed in Table 2 as has been reported for other nanoparticles such as quantum dots [27–29]. The triplet state lifetimes (τ_T) of the free MPc complexes are low ranging from 57 to 70 μs. With the exception of SnMCPc–GSH-AuNPs-mixed, the lifetimes increase in the presence of GSH-AuNPs (mixed or linked). The GeMCPc–GSH-AuNPs-linked conjugate gave the highest triplet quantum yield of 0.75 and the longest triplet lifetime of 130 μs. The triplet quantum yields and lifetimes are in the range of most

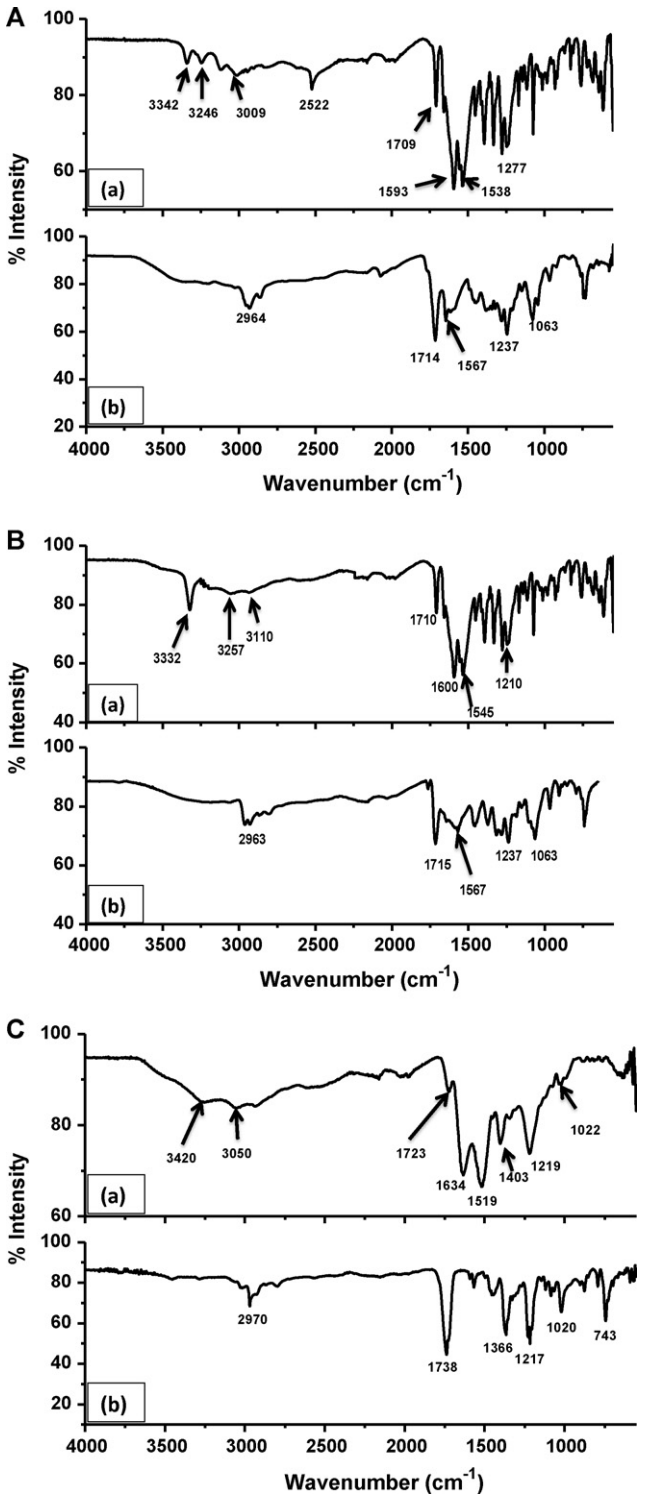

Fig. 4. Infrared spectra of Ge (A), Ti (B) and Sn (C), linked to nanoparticles (a) and Pc alone (b).

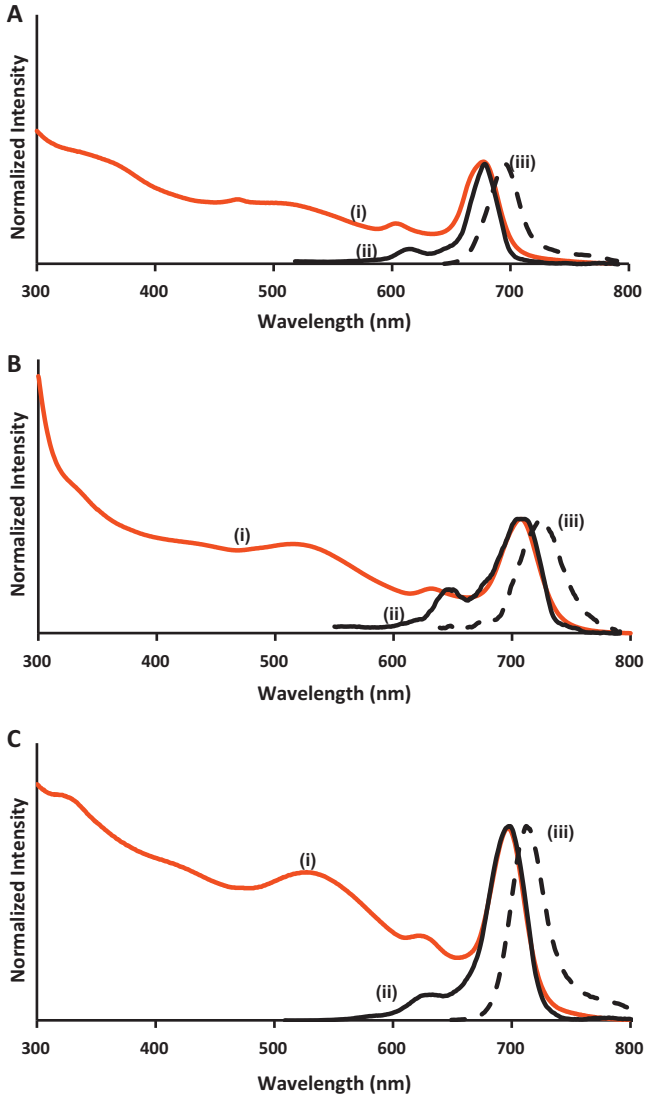

Fig. 5. Ground state absorption (i), fluorescence excitation (ii) and emission (iii) spectra of GeMCPc–GSH-AuNPs-linked (A), TiMCPc–GSH-AuNPs-linked (B) and SnMCPc–GSH-AuNPs-linked (C) in DMF.

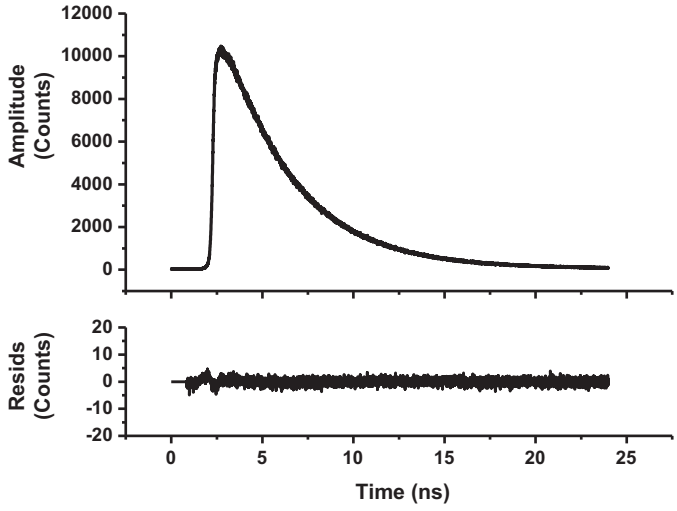

Fig. 6. Photoluminescence decay curve of TiMCPc–GSH-AuNPs-linked in DMF and the residuals of the fit.

germanium phthalocyanine complexes [30]. In homogeneous solutions, the observed triplet state lifetimes of phthalocyanines are dependent on a number of factors such as the nature of the solvent, the ground state concentration; the triplet state concentration and the presence of quenchers. The reduction in the exposure of the phthalocyanine sensitizer to the environment has been used to explain the increase in triplet lifetimes for phthalocyanines [31].

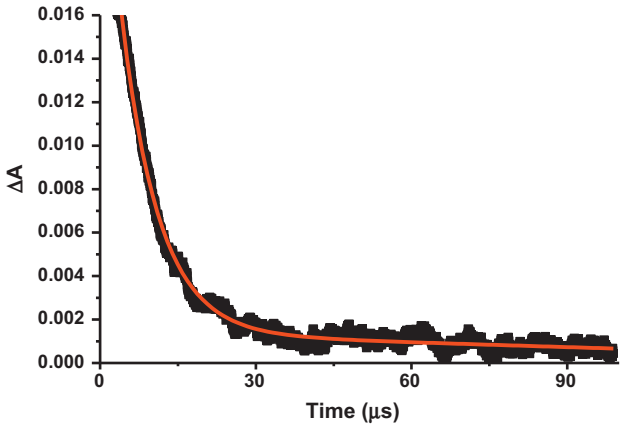

Fig. 7. Triplet decay curve of SnMCPc linked to GSH capped AuNPs in DMF.

This could explain the increase in triplet lifetimes in the presence of AuNPs.

4. Conclusions

Conjugation of phthalocyanine complexes to GSH-AuNPs resulted in blue shifting of the Q-band absorption spectra, confirming successful linking. Appearance of both nanoparticle and phthalocyanines XRD peaks and changes in the angle and d-spacing confirmed a new crystal form. A large improvement in the triplet lifetimes for the linked conjugate was observed for all the complexes. However conjugation resulted in low fluorescence quantum yields and lifetimes.

Acknowledgements

This work was supported by the Department of Science and Technology (DST)/Nanotechnology (NIC) and National Research Foundation (NRF) of South Africa through DST/NRF South African Research Chairs Initiative for Professor of Medicinal Chemistry and Nanotechnology and Rhodes University. NM thanks DAAD for funding.

Appendix A. Supplementary data

Supplementary data associated with this article can be found, in the online version, at doi:10.1016/j.jphotochem.2011.08.009.

References

[1] Z. Zhang, J. Jia, Y. Lai, Y. Ma, J. Weng, L. Sun, Bioorgan. Med. Chem. 18 (2010) 5528.
[2] M.-C. Daniel, D. Astruc, Chem. Rev. 104 (2004) 293.
[3] V. Biju, T. Itoh, A. Anas, A. Sujith, M. Ishikawa, Anal. Bioanal. Chem. 391 (2008) 2469.
[4] M. Pelton, J. Aizpurua, G. Bryant, Laser Photon. Rev. 2 (2008) 136.
[5] R. Bonnet, In Chemical Aspects of Photodynamic Therapy, Gordon and Breach Science Publishers, Amsterdam, 2000.
[6] R.R. Allison, G.H. Downie, R. Cuenca, X.H. Hu, C.J.H. Childs, C.H. Sibata, Photodiagn. Photodyn. 1 (2004) 27.
[7] D.C. Hone, P.I. Walker, R. Evans-Gowing, S. FitzGerald, A. Beeby, I. Chambrier, et al., Langmuir 18 (2002) 2985.
[8] M.E. Wieder, D.C. Hone, M.J. Cook, M.M. Handsley, J. Gavrilovic, D.A. Russel, Photochem. Photobiol. Sci. 5 (2006) 727.
[9] M. Camerin, M. Magaraggia, M. Soncin, G. Jori, M. Moreno, I. Chambrier, et al., Eur. J. Cancer 46 (201) (1910).
[10] A. Kotiaho, R. Lahtinen, A. Efimov, H.K. Metsberg, E. Sariola, H. Lehtivuori, et al., J. Phys. Chem. C 114 (2010) 162.
[11] K.S. Lokesh, V. Narayanan, S. Sampath, Microchim Acta 167 (2009) 97.
[12] M. Brust, M. Walker, D. Bethell, D.J. Schiffrin, R. Whyman, J. Chem. Soc. Chem. Commun. (1994) 801.
[13] N. Masilela, T. Nyokong, Dyes Pigments 91 (2011) 164.
[14] J.R. Lakowicz, Principles of Fluorescence Spectroscopy, Second ed., Kluwer Academic/Plenum Publishers, New York, 1999.
[15] S. Fery-Forgues, D. Lavabre, J. Chem. Ed. 76 (1999) 1260.
[16] A. Ogunsipe, J.Y. Chen, T. Nyokong, New J. Chem. 7 (2004) 822.
[17] J. Kossanyi, D. Chahraoui, Int. J. Photoenergy 2 (2000) 9.
[18] A. Meister, M.E. Anderson, Annu. Rev. Biochem. 52 (1983) 711.
[19] S. Sapra, D.D. Sarma, Pramana 65 (2005) 565.
[20] V.C. Verma, S.K. Singh, R. Solanki, S. Prakash, Nanoscale Res. Lett. 6 (2011) 16.
[21] A.W. Snow, J.R. Griffith, N.P. Marullo, Macromolecules 17 (1984) 1614.
[22] Z.-L. Yang, H. Chen, L. Cao, H.-Y. Li, M. Wang, Mater. Sci. Eng. B 106 (2004) 73.
[23] T. Nyokong, H. Isago, J. Phthalocyanines Porphyrins 8 (2004) 1083.
[24] M.G. Debacker, O. Deleplanque, B. Van Vlierberge, F.X. Sauvage, Laser Chem. 8 (1988) 1.
[25] J.A. Lacey, D. Phillips, Photochem. Photobiol. Sci. 1 (2002) 378.
[26] A. Grofcsilk, P. Baranyai, I. Bitter, V. Csokai, M. Kubinyi, K. Szegletes, et al., J. Mol. Struct. 704 (2004) 11.
[27] M. Idowu, T. Nyokong, J. Lumin. 129 (2009) 356.
[28] S. Moeno, T. Nyokong, Polyhedron 27 (2008) 1953.
[29] M. Idowu, T. Nyokong, J. Photochem. Photobiol. A: Chem. 188 (2007) 200.
[30] M. Idowu, T. Nyokong, J. Photochem. Photobiol. A Chem. 204 (2009) 63.
[31] M.S.C. Foley, A. Beeby, A.W. Parker, S.M. Bishop, D. Phillips, J. Photochem. Photobiol. B 38 (1997) 10.